

# Reconstructing Toponium using Recursive Jigsaw Reconstruction

Aman Desai , Amelia Lovison , Paul Jackson 

*Department of Physics The University of Adelaide North Terrace Adelaide SA 5005 Australia*

---

## Abstract

The results from the ATLAS and CMS experiment at the Large Hadron Collider indicate the existence of a top-quark pair bound state near the  $t\bar{t}$  threshold region. We present a method relying on Recursive Jigsaw Reconstruction to reconstruct the toponium bound state at the  $t\bar{t}$  threshold region. We propose incorporating two variables in the analysis that can improve sensitivity to the toponium signal. Our results indicate that this method may be useful to gain additional insights into the physics phenomenology of the  $t\bar{t}$  threshold region.

*Keywords:* Toponium Physics

---

## 1. Introduction

The excess of events observed by the ATLAS and CMS experiments at the Large Hadron Collider (LHC), near the  $t\bar{t}$  pair production threshold in the dileptonic decay mode, is consistent with a spin-0 pseudo-scalar, toponium [1, 2, 3, 4, 5]. ATLAS found a local significance of  $7.7\sigma$  for this excess [3]. The reconstruction of the  $t\bar{t}$  dileptonic final state is challenging owing to the presence of two neutrinos in the final state that escape the detector without detection. The ATLAS and CMS experiments employ the Ellipse Method [6] and the Sonnechain Method [7, 8], respectively for reconstruction in their analyses. We present the use of the Recursive Jigsaw Reconstruction method [9] in this context, as a strategy for distinguishing the toponium signal from the background  $t\bar{t}$  events.

## 2. Monte Carlo Simulation and Event Preselection

The Monte Carlo samples used in this study were generated as per the LHC Run 3 configuration, that is, considering a centre-of-mass (CoM) energy of  $\sqrt{s} = 13.6$  TeV. Moreover, all samples were scaled according to the Run 3 integrated luminosity of  $\mathcal{L} = 300 \text{ fb}^{-1}$ . We simulated toponium samples according to the prescription given in [10] which reweights matrix elements using Non-Relativistic QCD Green's function. The hard scattered matrix elements

---

*Email addresses:* [aman.desai@adelaide.edu.au](mailto:aman.desai@adelaide.edu.au) (Aman Desai )  
[amelia.lovison@adelaide.edu.au](mailto:amelia.lovison@adelaide.edu.au) (Amelia Lovison )  
[p.jackson@adelaide.edu.au](mailto:p.jackson@adelaide.edu.au) (Paul Jackson )

are simulated in `MADGRAPH5_AMC@NLO` [11] and `PYTHIA8` [12] is used for hadronisation. The generation of  $t\bar{t}$  background events follows the use of `MADGRAPH5_AMC@NLO`, `MADSPIN` [13], and `PYTHIA8`. Two million signal samples and four million background samples were generated. We set the top quark mass to 173 GeV and the width to  $\Gamma_t = 1.49$  GeV.

To reconstruct the jets, we use the anti- $k_T$  algorithm [14] implemented within `FASTJET` [15] with a radius parameter of  $R = 0.4$ . The `FastJet` software is accessed via the `MadAnalysis5` [16, 17] framework. The normalisations for  $t\bar{t}$  and toponium are  $\sigma_{t\bar{t}} \times Br(W \rightarrow l\nu)^2 = 43.6$  pb [18, 19] and  $\sigma_\eta \times Br(W \rightarrow l\nu)^2 = 0.277$  pb, respectively.

We select events which consist of at least two oppositely charged leptons ( $ee, \mu\mu, e\mu$ ) and at least two bottom quark initiated jets ( $b$ -jets). A list of pre-selection criteria applied on the samples are summarised in Table 1.

Table 1: Pre-selection criteria used in this analysis.

Selection	Requirement
b-jet multiplicity	$N_{b-jet} \geq 2$
Lepton multiplicity	$N_\ell = 2$ with $\sum_\ell N_Q = 0$
b-jet $p_T$	$p_T^{b-jet} > 25$ GeV
b-jet $\eta$	$ \eta ^{b-jet} < 2.5$
Lepton $p_T$	$p_T^\ell > 25$ GeV
Lepton $\eta$	$ \eta ^\ell < 2.5$
$\Delta R(b\text{-jet}, \text{Lepton})$	$\Delta R(b\text{-jet}, \ell) > 0.4$

### 3. Reconstruction Method for $t\bar{t}$ in Dilepton Final States

In this study, the reconstruction of  $t\bar{t} \rightarrow bbW(l\nu)W(l\nu)$  is implemented in the `RestFrames` package which is based on the Recursive Jigsaw Reconstruction method [9]. The reconstruction is challenging owing to both - pairing  $b$ -jet with the leptons (combinatoric challenge) and to deal with unmeasured particles (two neutrinos). The algorithm first chooses a decay tree that considers all intermediate particle decays with visible and invisible final state particles. Then for each step in the decay tree, it applies a jigsaw rule relating the current frame of reference to the next as a function of kinematic variables. These steps are then applied recursively until it reaches the end of the decay chain. The decay tree used in this analysis is shown in Figure 1.

We apply this Recursive Jigsaw Reconstruction technique [9] via the use of the `RestFrames` package. There are four different ways in which the dilepton  $t\bar{t}$  system can be constrained. These constraints formulate the following methods:

- A:**  $M_{\text{top}}^a = M_{\text{top}}^b$
- B:**  $M_W^a = M_W^b$
- C:**  $\min \Sigma M_{\text{top}}^2$
- D:**  $\min \Delta M_{\text{top}}$

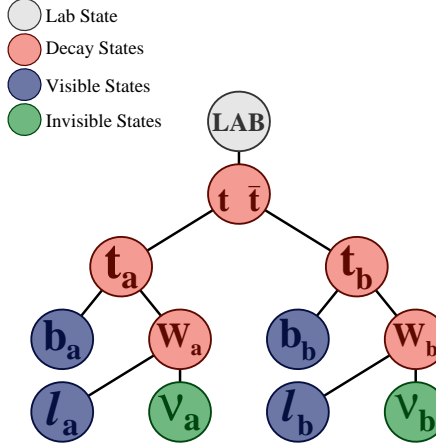


Figure 1: Example decay tree diagram of the process  $t\bar{t} \rightarrow b\bar{b}W(l\nu_l)W(l\nu_l)$

As shown in Figure 2, reconstruction method A is the optimal method, allowing for the most consistent top mass.

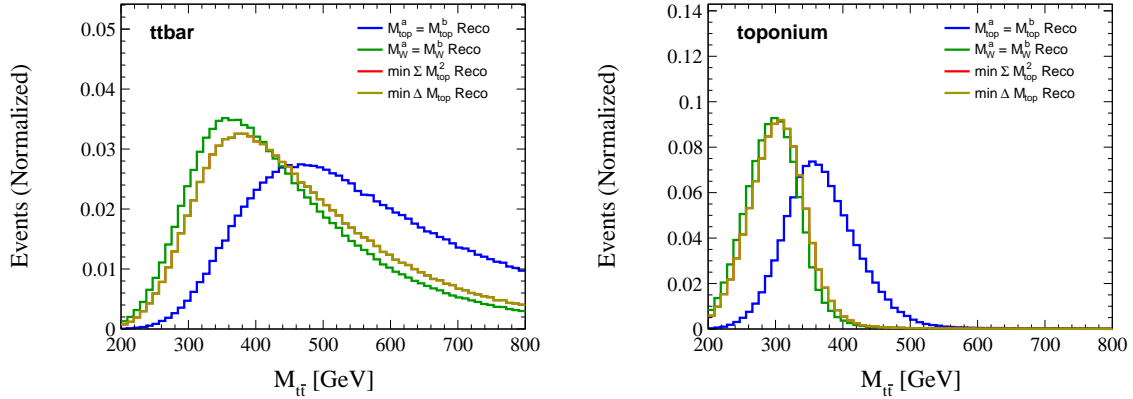


Figure 2: Invariant mass distributions of the top-quark pair as evaluated by the reconstruction algorithms.

#### 4. Analysis

In this study, we present two variables that can improve the sensitivity for the toponium analysis in the  $t\bar{t}$  dilepton final state. This includes  $\Delta\phi(t\bar{t})$  which is the difference in azimuthal angle of a reconstructed top quark pair, and  $N_{\text{chel}}$  which is defined as the scalar product of the lepton's momenta obtained by first boosting the lepton to the  $t\bar{t}$  CoM frame of reference and then boosting it to the parent top-quark frame. In this procedure the top quark is not boosted to the CoM frame. As shown in Figure 3, the parton-level distributions are presented for these

variables for both the  $t\bar{t}$  and toponium samples. Both exhibit quite distinctive behaviour that differs between the signal and the background. The correlations between the  $\Delta\phi(t\bar{t})$  and  $N_{chel}$  variables are presented in Figure 4.

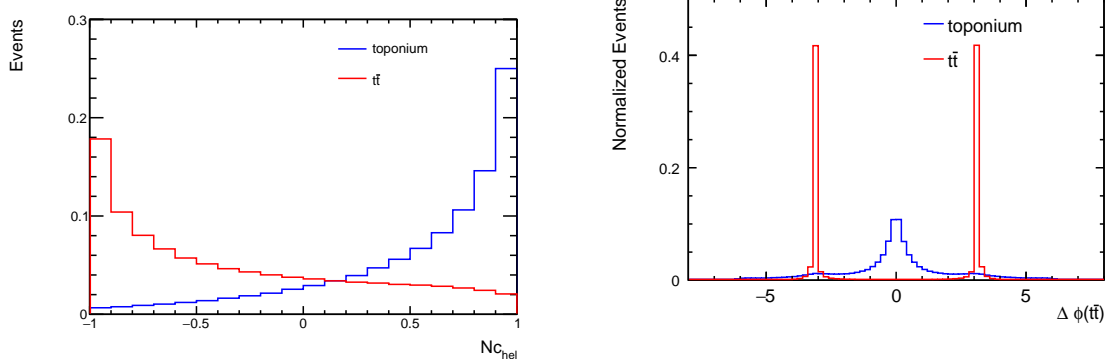


Figure 3: Truth level distributions for  $\Delta\phi(t\bar{t})$  and  $N_{chel}$  variables.

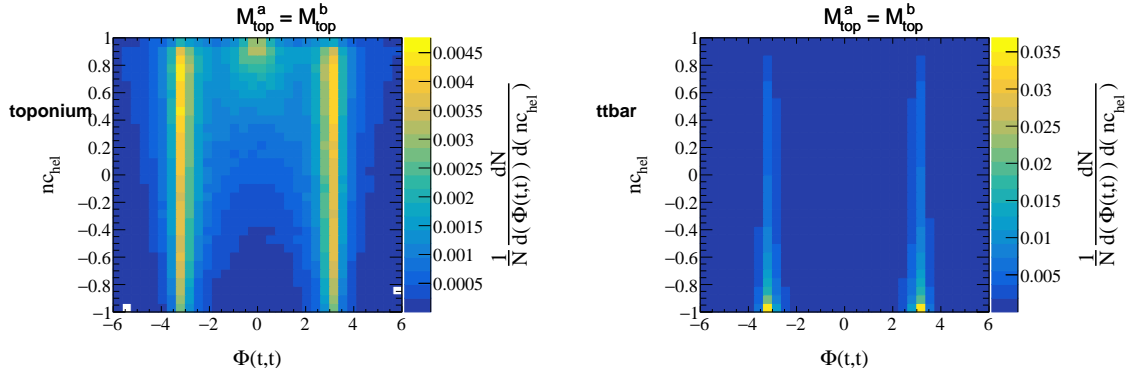


Figure 4: Correlation between the  $\Delta\phi(t\bar{t})$  and  $N_{chel}$  variables for Toponium sample (left) and  $t\bar{t}$  sample (right).

Nine regions are constructed in the phase space of the  $\Delta\phi(t\bar{t})$  and  $N_{chel}$  variables. The bins considered are as follows:

$$\begin{aligned} \Delta\Phi(t\bar{t}) &\in \{[-6, -2], [-2, 2], [2, 6]\}; \\ N_{chel} &\in \{[-1, -0.4], [-0.4, 0.4], [0.4, 1]\}; \\ \mathcal{R} &= \Delta\Phi(t\bar{t}) \text{bins} \otimes N_{chel} \text{bins}. \end{aligned}$$

The significance metric is defined as  $\frac{S}{\sqrt{S+B}}$ , where  $S$  represents the toponium yield and  $B$  represents the  $t\bar{t}$  yield. We use the observable  $M_{t\bar{t}}$  to evaluate the significance, and the results are presented in Figure 5.

As a result of identifying the optimal region defined as  $\Delta\phi(t\bar{t}) \in [-2, 2]$  and  $N_{chel} \in [0.4, 1]$ , the  $M_{t\bar{t}}$  distribution is shown in Figure 5 and the significance achieved in this region is  $15.3\sigma$ .

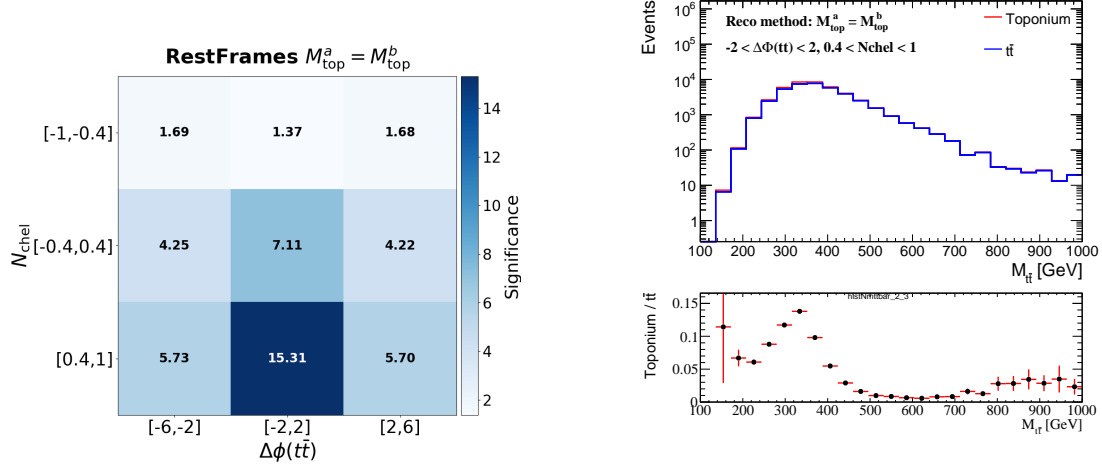


Figure 5: Results after pre-selections. (a) Significance obtained in the nine analysis regions. (b) Reconstructed  $t\bar{t}$  invariant mass in the optimal region.

## 5. Conclusion

We have presented the Recursive Jigsaw Reconstruction method as an improved strategy for reconstructing the quasi-bound state toponium, at the Large Hadron Collider, considering the CoM energy of the Run 3 configuration. Within this analysis strategy we have introduced one variable and identified another, being  $N_{chel}$  and  $\Delta\phi(t\bar{t})$ , which show that they are effective in discriminating toponium from the  $t\bar{t}$  background. In the phase space defined as  $\Delta\phi(t\bar{t}) \in [-2, 2]$  and  $N_{chel} \in [0.4, 1]$  we achieved a significance of  $15.3\sigma$ .

## References

- [1] V. S. Fadin and V. A. Khoze, Threshold Behavior of Heavy Top Production in  $e^+e^-$  Collisions, JETP Lett. **46** (1987) 525.
- [2] V. S. Fadin, V. A. Khoze and T. Sjöstrand, On the Threshold Behavior of Heavy Top Production, Z. Phys. C **48** (1990) 613. doi:10.1007/BF01614696.
- [3] ATLAS Collaboration, Observation of a cross-section enhancement near the  $t\bar{t}$  production threshold in  $\sqrt{s} = 13$  TeV pp collisions with the ATLAS detector, ATLAS-CONF-2025-008.
- [4] CMS Collaboration, Search for heavy pseudoscalar and scalar bosons decaying to a top quark pair in proton-proton collisions at  $\sqrt{s} = 13$  TeV, arXiv:2507.05119.

- [5] CMS Collaboration, Observation of a pseudoscalar excess at the top quark pair production threshold, *Rept. Prog. Phys.* **88** (2025) 087801. [doi:10.1088/1361-6633/adf7d3](https://doi.org/10.1088/1361-6633/adf7d3).
- [6] B. A. Betchart, R. Demina and A. Harel, Analytic solutions for neutrino momenta in decay of top quarks, *Nucl. Instrum. Meth. A* **736** (2014) 169–178. [doi:10.1016/j.nima.2013.10.039](https://doi.org/10.1016/j.nima.2013.10.039).
- [7] L. Sonnenschein, Algebraic approach to solve  $t\bar{t}$  dilepton equations, *Phys. Rev. D* **72** (2005) 095020. [doi:10.1103/PhysRevD.72.095020](https://doi.org/10.1103/PhysRevD.72.095020).
- [8] L. Sonnenschein, Analytical solution of  $t\bar{t}$  dilepton equations, *Phys. Rev. D* **73** (2006) 054015; Erratum *Phys. Rev. D* **78** (2008) 079902.
- [9] P. Jackson and C. Rogan, Recursive Jigsaw Reconstruction: HEP event analysis in the presence of kinematic and combinatoric ambiguities, *Phys. Rev. D* **96** (2017) 112007. [doi:10.1103/PhysRevD.96.112007](https://doi.org/10.1103/PhysRevD.96.112007).
- [10] B. Fuks, K. Hagiwara, K. Ma and Y.-J. Zheng, Simulating toponium formation signals at the LHC, *Eur. Phys. J. C* **85** (2025) 157. [doi:10.1140/epjc/s10052-025-13853-3](https://doi.org/10.1140/epjc/s10052-025-13853-3).
- [11] J. Alwall *et al.*, The automated computation of tree-level and next-to-leading order differential cross sections, and their matching to parton shower simulations, *JHEP* **07** (2014) 079. [doi:10.1007/JHEP07\(2014\)079](https://doi.org/10.1007/JHEP07(2014)079).
- [12] C. Bierlich *et al.*, A comprehensive guide to the physics and usage of PYTHIA 8.3, *SciPost Phys. Codebases* **2022** (2022) 8. [doi:10.21468/SciPostPhysCodeb.8](https://doi.org/10.21468/SciPostPhysCodeb.8).
- [13] P. Artoisenet *et al.*, Automatic spin-entangled decays of heavy resonances in Monte Carlo simulations, *JHEP* **03** (2013) 015. [doi:10.1007/JHEP03\(2013\)015](https://doi.org/10.1007/JHEP03(2013)015).
- [14] M. Cacciari, G. P. Salam and G. Soyez, The anti- $k_t$  jet clustering algorithm, *JHEP* **04** (2008) 063. [doi:10.1088/1126-6708/2008/04/063](https://doi.org/10.1088/1126-6708/2008/04/063).
- [15] M. Cacciari, G. P. Salam and G. Soyez, FastJet User Manual, *Eur. Phys. J. C* **72** (2012) 1896. [doi:10.1140/epjc/s10052-012-1896-2](https://doi.org/10.1140/epjc/s10052-012-1896-2).
- [16] E. Conte and B. Fuks, Confronting new physics theories to LHC data with MADANAL-YSIS 5, *Int. J. Mod. Phys. A* **33** (2018) 1830027. [doi:10.1142/S0217751X18300272](https://doi.org/10.1142/S0217751X18300272).
- [17] J. Y. Araz, B. Fuks and G. Polykratis, Simplified fast detector simulation in MADANAL-YSIS 5, *Eur. Phys. J. C* **81** (2021) 329. [doi:10.1140/epjc/s10052-021-09052-5](https://doi.org/10.1140/epjc/s10052-021-09052-5).
- [18] ATLAS Collaboration, Measurement of the  $t\bar{t}$  cross section and its ratio to the  $Z$  production cross section using pp collisions at  $\sqrt{s} = 13.6$  TeV, *Phys. Lett. B* **848** (2024) 138376. [doi:10.1016/j.physletb.2023.138376](https://doi.org/10.1016/j.physletb.2023.138376).
- [19] CMS Collaboration, First measurement of the top quark pair production cross section in proton-proton collisions at  $\sqrt{s} = 13.6$  TeV, *JHEP* **08** (2023) 204. [doi:10.1007/JHEP08\(2023\)204](https://doi.org/10.1007/JHEP08(2023)204).